

Computational Modeling of Organic Rankine Cycle Combined Heat and Power for Sedimentary Geothermal Exploitation

Nicholas Fry^{1,2,4}, Jessica Eagle-Bluestone¹, and Francesco Witte³

¹University of North Dakota Institute of Energy Studies

²Harold Hamm School of Geology and Geological Engineering

³German Aerospace Center (DLR), Institute of Networked Energy Systems

⁴Egg Geo LLC

Keywords

Simulation, combined heat and power, sedimentary geothermal, thermal networks

ABSTRACT

Research of geothermal potential across the Williston Basin indicates relatively low temperatures near the Precambrian basement. These temperature estimates vary by distance from the middle of the Basin but are assumed to be between about 120-150° at center. Near the Basin center are several rural communities and small towns. Often these small towns are adjacent to the Missouri River, including Lake Sakakawea.

By combining low-temperature geothermal fluids with an Organic Rankine Cycle (ORC), cooling fluids from the Missouri River, and thermal demands from New Town, North Dakota – a community on the shores of Lake Sakakawea – it is possible to maximize the utilization rate of sedimentary geothermal energy. In this desktop study, we build on the work of others who suggest the thermo-economic optimum for low temperature combined heat and power (CHP) plants require a form of heat exchange in parallel with an ORC preheater, after the heat transfer in an evaporator. We are extending this concept by implementing a heat source matching strategy for the structures in New Town, in combination with the CHP-ORC.

Beginning with programming the CHP-ORC configuration in Thermal Engineering Systems in Python (TESPy), then extracting an array of power outputs at each heat exchange point, we run two design constraints for the thermal network using a spatially accurate topology in Comsof Heat. We briefly consider the economics as part of ongoing research. The outcome is an early implementation of simulations for the function and operation of low temperature geothermal heating and power across the Williston Basin.

1. Introduction

Previous investigations of distributed geothermal power plants along the Missouri River indicate the reservoir would be useful as a cooling source, eliminating cooling towers, and improving the production capacity using low-temperature fluids (<150°) (W. Gosnold et al., 2017). There are additional considerations that require scrutiny of this concept, including the release of high temperature effluents back to the Missouri River, permitting, among others. Assuming the outcomes are favorable, this type of distributed geothermal generation may be particularly helpful for residents of the Fort Berthold Indian Reservation along the Missouri River. Fort Berthold Indian Reservation is an area above the Williston Basin with very active oil and gas operations, exploiting the Bakken Formation. Since the Reservation is adept at subsurface exploitation, a geothermal energy transition may be within reach if a repeatable workflow for power plant and thermal network feasibility is available. The following is an attempt to find and release that workflow for public implementation.

1.1 Power Production from Low-enthalpy Geothermal Resources

The Organic Rankine Cycle (ORC) is a common power production cycle for low-enthalpy waste heat streams, such as those found downstream in industrial processes, and marine power applications on seafaring vessels. Likewise, ORC is a power cycle well-suited for the exploitation of low-enthalpy geothermal fluids. The Kalina cycle is another binary power cycle available from waste-to-power manufacturers.

Geothermal resources of moderate enthalpy also use ORC power plants. Moderate enthalpy resources, however, are geographically limited by comparison to low-enthalpy resources. In the United States, a common setting for low-enthalpy geothermal resources are sedimentary basins. Sedimentary basin aquifers entrap and limit convective heat flow in confined and semi-confined layers. These stratigraphic limitations on convective fluid flow often result in advective heat flow. This advective heat flow is readily accessible by vertical or horizontal wells, depending on the porosities, permeabilities, and stress regimes at depth, as well as the needs of the power cycle at the surface (W. D. Gosnold et al., 2012).

1.2 Heat and Power Production from Low-enthalpy Geothermal Resources

Adding a heat demand to an ORC unit has thermodynamic implications that affect the exergo-economics of the power plant in place (Habka & Ajib, 2014). Putting a heat demand on a power cycle of any kind introduces a “security of supply” problem. That heat demand is very likely to take priority over the power production. Often end-users are residential-commercial service areas and there is no room for heat blackouts in the dead of winter across temperate or cold regions of the world. The less geographically limited low-enthalpy geothermal resources open the opportunity to use ORC combined heat and power (CHP) plants in many of these temperate or cold regions, including North Dakota. CHP-ORC for geothermal resources in these regions, therefore, requires careful consideration, simulation, sensitivity analysis, and risk mitigation strategies.

Previous investigations of CHP-ORC indicate heat demands have two principal effects on the power cycle. In the first case, the demand robs the power production cycle by diverting flow to a lower grade of energy. Direct uses of heat, though more energetically efficient, are a lower grade of energy end use. In contrast, electricity production from the ORC is a high grade of energy –

capable of very long-distance transmission and an increasing number of industrial applications that require it. In the second case, a higher heat source temperature, though beneficial for electricity generation, will incur more extreme heat losses when coupled to a heat demand.

1.3 Advanced Geothermal District Energy Networks

District energy systems (DES) are “energy agnostic.” Energy agnosticism allows the thermal network to transfer energy from a variety of heat sources and sinks. Traditional steam district heating (DH) networks were first developed in New York, by Birdsill Holly in the late 1800s (Collins, 1959). The Holly Steam Combination Company used buried steam conduits connected to a centralized boiler unit. This style of district energy became very popular, now being known as “first generation district heating” (Lund et al., 2014).

Later came hot water distribution networks below 100°. Through the 1960s the popularity of these networks declined due to cheap fossil energy production and expansive electric grids. District energy saw a spurt of growth through the 1970s oil crises. Preinsulated, direct burial steel lines demark the third generation of DH (Frederiksen & Werner, 2013). The highest market penetration for third generation district heating took place across the Nordic countries, including Sweden – a country without domestic oil or gas production.

A history of high fossil fuel costs also coincides with geothermal district energy network construction in the United States. Unlike the United States, however, Sweden did not stop installing district energy networks following the return to normal fossil fuel costs in the 1980s (Werner, 2017). As a result of continuous regulated installation of district energy networks, Sweden balanced their foreign trade deficit, reabsorbing gross domestic product and decoupling economic resilience from fossil fuel consumption levels (Lövin & Andersson, 2015). Sweden no longer uses fossil fuels for their building heating and cooling demands. Now deregulated energy service companies, providing centralized and distributed waste heats, make up a sustainable industry that exports Swedish pipeworks and expertise to other companies and countries seeking energy efficiency.

Although Frederiksen & Werner wrote the contemporary standard of DH and cooling in 2013, by 2014 Lund et al. wrote modern descriptions of “fourth generation district energy.” Modern district energy networks provide opportunities for distributed energy applications, including thermal energy storage, prosumerism, and drastic reductions in primary energy consumption. Temperatures across fourth generation district energy networks are below 60-70°. Energy sources may be centralized or distributed. Many optimizations of the lower temperature networks are the result of substation placements, heat recovery, advanced control systems, and digitization of engineering through operational processes (Averfalk et al., 2021).

Lower temperature thermal networks, in combination with a power station, may also improve the efficiency of the electricity generating power cycle. By reducing the return temperatures from a thermal network, the condenser of the generator set can benefit. Whether it is the reduction in thermal losses, the implementation of lower MHGC sources of renewable energy, or the improvement in electricity generation, advanced district energy technology contributes to the cost reduction gradient (CRG). These methods for reducing primary energy consumption are yet to be exploited, either in the United States or abroad (Averfalk et al., 2021).

Advanced geothermal DES leverage two primary energy efficiency advantages. Firstly, they offset the need for major electricity allocations for heating and cooling. They do so by either using geothermal fluids in a direct heat transfer mode or combine that heat transfer with an additional compression cycle – or heat pump – to decrease the thermal energy input to output ratio. Secondly, when the systems themselves couple with thermal energy storage, the micro-grid can become a demand-side management tool to ameliorate electricity generation requirements at connected power plants. Thermal energy storage in combination with geothermal energy exploitation in these distributed thermal energy networks is highly advantageous, reducing the overall distribution pipe size (van der Heijde et al., 2019; Jebamalai et al., 2020).

Most electrification projects for remote and rural communities have been based on solar/wind (White Hawk, 2017). An advantage of geothermal-based thermal networks is that they do not rely on intermittent solar and wind sources. As such the integration and controls of geothermal DES are less complex. The required power electronics controllers in such systems should be less complex compared to those in solar/wind-based DES. Solar/wind systems need expensive battery energy storage to mitigate their intermittent nature of energy supply. Electric battery storage is also resource extractive, with a greater environmental impact than hot or cold fluid storage used in geothermal districts. These advantages, in comparison to solar/wind DES, make geothermal-based thermal networks more energetically attractive.

1.4 Implementation of ORC-CHP in Practice

From this brief review, an effective ORC-CHP implementation should be close to the point of heat demands, the thermal network should be as temperature agnostic as possible and placing a priority on electricity generation will improve the exergo-economics, implying a more remunerative power project.

1.5 Description of Case Study Site – New Town, North Dakota

New Town, North Dakota is on the Fort Berthold Indian Reservation in the west-central region of the state (see page 13 for site map). Fort Berthold Indian Reservation is home to the Mandan, Hidatsa, and Arikara (MHA) Nation. In 1851 Chief Four Bears, founder of the integrated MHA village, Like-a-Fishhook, signed a treaty with the US Government, establishing the Reservation. In 1953, the US Government forced the removal of the Three Affiliated Tribes from the towns and farms along the Missouri River during the installation of the Garrison Dam. By 1954, New Town, North Dakota became a settlement for displaced residents of now flooded municipalities, Elbowoods, Sanish, and Van Hook (State Historical Society of North Dakota, 2020).

This case study asks the following questions:

How much electricity and thermal can be offset with deep geothermal production fluids and an ORC in the Williston Basin?

What are the point emissions reductions using an CHP-ORC, compared to incumbent propane and electricity from North Dakota grid?

2. Methods

This section will introduce the methods applied in this study. First, the power plant simulation setup is described, followed by the geothermal reservoir modeling. Lastly, the methods to model heat demand and heat distribution in a DH system are presented.

2.1 Power Plant Model

The simulation of thermal conversion processes is a fundamental and well-known discipline in engineering. A simulation is usually carried out by setting up a model for each unit, e.g., heat exchangers, turbines, pumps or valves, in a process and connecting these units to form a topological network. The network and its parameters can then be represented in a mathematical model, which can be solved using appropriate algorithms. In this study, the thermal conversion process model will be simulated with the open-source software TESPpy, which allows the user to lay out a process with generic topology and simulate steady-state operation in both, design and part-load operation (Witte & Tuschy, 2020). More information on the software can be found in the extensive online documentation at <https://tespy.readthedocs.io>.

In an ORC-CHP there are different possibilities to make use of the geothermal energy to provide heat and electricity simultaneously. For example, the geothermal source can provide heat to the ORC and then transfer it to the heating network by further reducing the temperature of the geothermal brine in a series configuration. A second location for heat transfer could be from a preheater in parallel with the ORC evaporator in a parallel configuration (Habka & Ajib, 2014; Van Erdeweghe et al., 2018). In this project the hybrid parallel configuration (Figure 1) known as the “Habka 4” is selected, because of its history of rigorous simulation using a variety of power plant and fluid dynamics simulation engines. To make these simulations more available for future users, an open GitHub repository¹ is available to run this generator set under alternative geothermal fluid production parameters, lake temperatures, among others.

In the configuration, the geothermal production well provides heat to the evaporator of the ORC power cycle. Downstream the mass flow splits up. One part preheats the working fluid, the other part transfers heat to the DES in the DH heat exchanger. Both streams merge again and are reinjected at a lower temperature into the subsurface reservoir. Due to the high concentration of minerals in the geothermal brine at the Williston Basin, the reinjection temperature is constrained to a minimum value of 90°C to prevent precipitation in the heat exchangers or in the reinjection bore hole for this case study. Therefore, values 24 and 26 are restricted to 90°C.

Calculation of the evaporation pressure of the working fluid inside the ORC power cycle is based on heat demand specification. The plant operates with Isopentane as a working fluid. The relationship between design heat demand and evaporation pressure as well as power generation is shown in Figure 2. The condenser of the geothermal ORC discharges the waste heat into a lake. In the model, the lake pump is controlled in a way that the outflow temperature is 10°C higher than the lake temperature. Selected design parameters of the process are listed in Table 1.

¹ https://github.com/fwitte/chp_orc

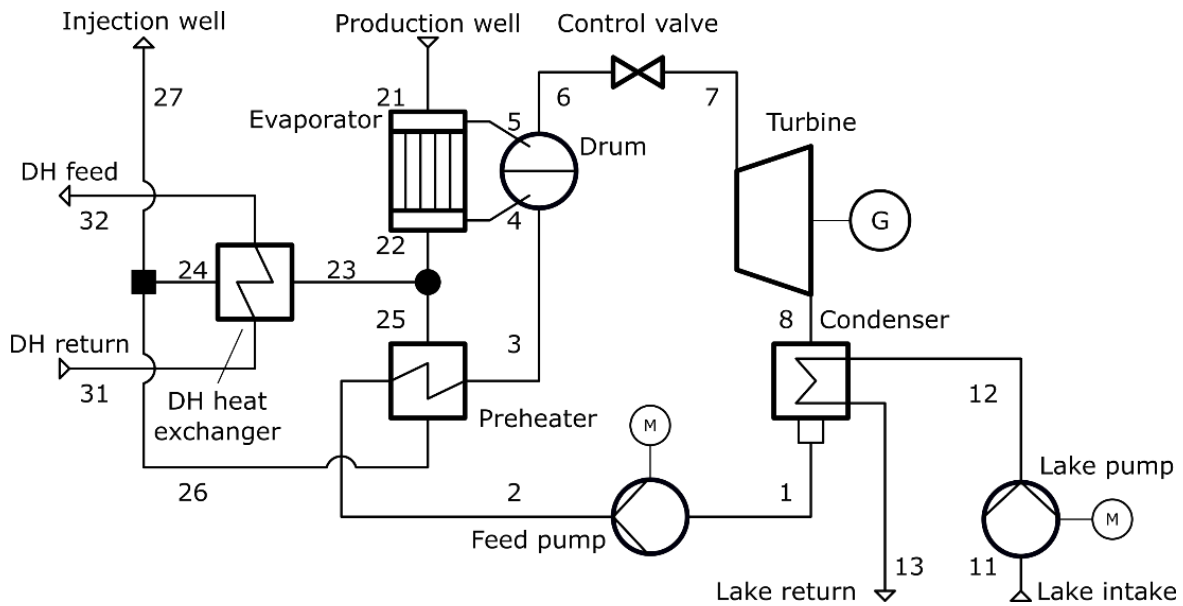


Figure 1 Organic Rankine Cycle with DH connections, modified from: Sarah Van Erdeeweghe et al. (2018).

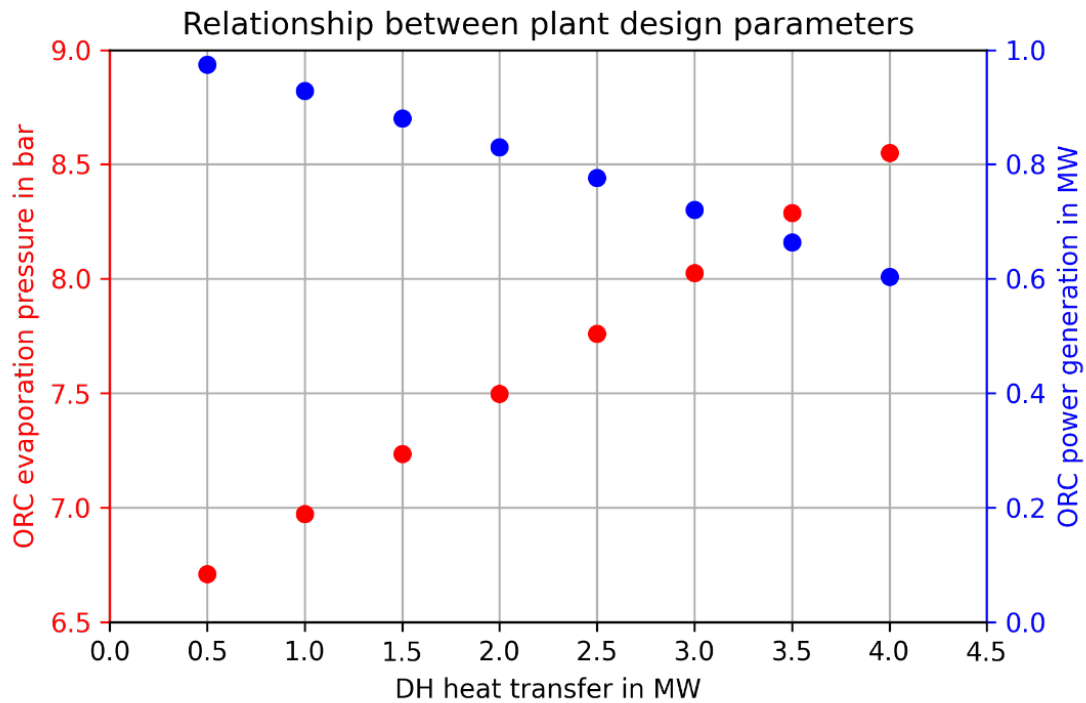


Figure 2 Dependency of power production and evaporation pressure of the working fluid to the heat transfer in the DH heat exchanger.

Table 1 Overview on selected design parameters of the ORC-CHP system.

Label	Parameter	Symbol	Value	Unit
turbine	efficiencies (isentropic, electric-mechanical)	$\eta_{is}\eta_{el,m}$	90, 97	%
pumps	efficiencies (isentropic, electric-mechanical)	$\eta_{is}\eta_{el,m}$	75, 97	%
condenser	temperature difference	$T_1 - T_{13}$	10	°C
	pressure ratio hot side	pr	1	-
evaporator	pinch point	$T_{22} - T_5$	10	°C
	pressure ratio cold side	pr	1	-
preheater	approach point	$T_{4,sat} - T_4$	3	°C
heat exchangers	pressure ratios	pr	0.98	-
lake water	temperature increase	$T_{13} - T_{11}$	10	°C
production well	temperature	T_{21}	130	°C
injection well	temperature	T_{24}, T_{26}	90	°C

The part-load operation of the plant is simulated by applying characteristic curves for the efficiency of heat transfer and turbines as well as pumps. The temperatures 24 and 26 are fixed to the minimum reinjection temperature. However, in case the ORC power cycle is overloaded, the temperature value 26 can increase to values higher than the minimum reinjection temperature. This occurs when the working fluid mass flow increases with lower heat demand. The turbine then requires a higher pressure at the inlet to deal with the increased mass flow. This finally results in a pressure ratio larger than 1 in the control valve, which is physically impossible. In those instances, the model sets the valve's pressure ratio to 1 (valve is completely opened) in lieu of setting the temperature at 26 to 90°C.

By always keeping the temperature 24 value constant at 90°C, the feed temperature of the DH system cannot be controlled within the DH heat exchanger anymore. However, partially bypassing the heat exchanger and mixing the cold return flow with the excess heating feed flow from the heat exchanger, the temperature value can be brought down to the appropriate level without changing the overall heat input. The DH water circulation is therefore increased. Since this does not affect the operation of the ORC system, it is not part of the simulation. Employing this strategy, the DH system temperature does not influence the other components of the plant.

Traditional definitions of electrical, thermal, and overall efficiency apply at the CHP-ORC. An electrical efficiency factor (η_{elec}) at the plant is Equation 1. Thermal efficiency (η_{th}) at the point of the DH heat exchanger is given by Equation 2. Overall efficiency (η_{tot}) is the sum (Equation 3). Determining the production allocation (A_H) for the heat follows Equation 4, and power allocation (A_P) appears in Equation 5.

$$\eta_{elec} = \frac{P_{out}}{Q_{in}} \quad \text{Equation 1}$$

$$\eta_{th} = \frac{H_{out}}{Q_{in}} \quad \text{Equation 2}$$

$$\eta_{\text{tot}} = \eta_{\text{th}} + \eta_{\text{elec}} \quad \text{Equation 3}$$

$$A_H = H_{\text{out}} / (H_{\text{out}} + P_{\text{out}}) * 100\% \quad \text{Equation 4}$$

$$A_P = P_{\text{out}} / (H_{\text{out}} + P_{\text{out}}) * 100\% \quad \text{Equation 5}$$

2.2 Geothermal Resource Characteristics

The Williston Basin forms the southeastern extremity of the Western Canada Sedimentary basin. It is an intracratonic Phanerozoic basin, comprised of six stratigraphic sequences, bounded by major unconformities. The basin covers an area of 250,000 km², has a diameter of 560 km and a maximum thickness of 4900m. While it extends into eastern Montana, South Dakota, Manitoba and Saskatchewan the ellipsoidal depression is centered in North Dakota (Kent & Christopher, 1994).

m/A Thermal Drawdown Parameter Model

Equation 6 is available in GEOPHIRES to calculate the transient reservoir production temperature. The reservoir is represented as a single rectangular fracture of specified area with a uniform liquid flow over the fractured surface (Armstead & Tester, 1987; K. F. Beckers & McCabe, 2019).

$$T_{WD} = \frac{T_W - T_{W, \text{inlet}}}{T_{R,0} - T_{W, \text{inlet}}} = \text{erf} \left(\frac{1}{A} \frac{1}{m} c_W \sqrt{\frac{k_R \rho_R c_R}{t}} \right) \quad \text{Equation 6}$$

Where:

erf = error function

t = time in seconds

T_{WD} = Water temperature (°C)

T_{R,0} = initial reservoir temperature (°C)

c_W = specific heat capacity of water

k_R = rock thermal conductivity

ρ_R = rock density

c_R = Rock specific heat capacity

m/A = mass loading parameter, defined as mass flow rate per unit area of a single fracture

T_{W,inlet} = water temperature at the reservoir inlet (°C)

There are several ways to assess the temperature at depth from sedimentary basins. Using the bottom hole temperature in well logs is not appropriate, as the log measurements are taken before the borehole heats up again, following the cooling by drilling fluids. Two general methods are

the Harrison correction and thermostratigraphy (TSTRAT). The Harrison bottom hole temperature (BHT) correction was modified in 2004 from its original 1983 form (Blackwell & Richards, 2004). An example of the Harrison correction appears in Equation 7, where Z is the depth. Using Deadwood Formation well data from (Namie et al., 2022), ordinary kriging of the New Town area appears in Figure 3. Bootstrap simulation of the same temperature regime appears in Figure 4. A TSTRAT temperature interpretation formula appears in Equation 8.

$$T_{cf} = -16.51213476 + 0.01826842109 * Z - (2.344936959E - 006) * Z^2 \quad \text{Equation 7}$$

Where:

Z = Depth in meters

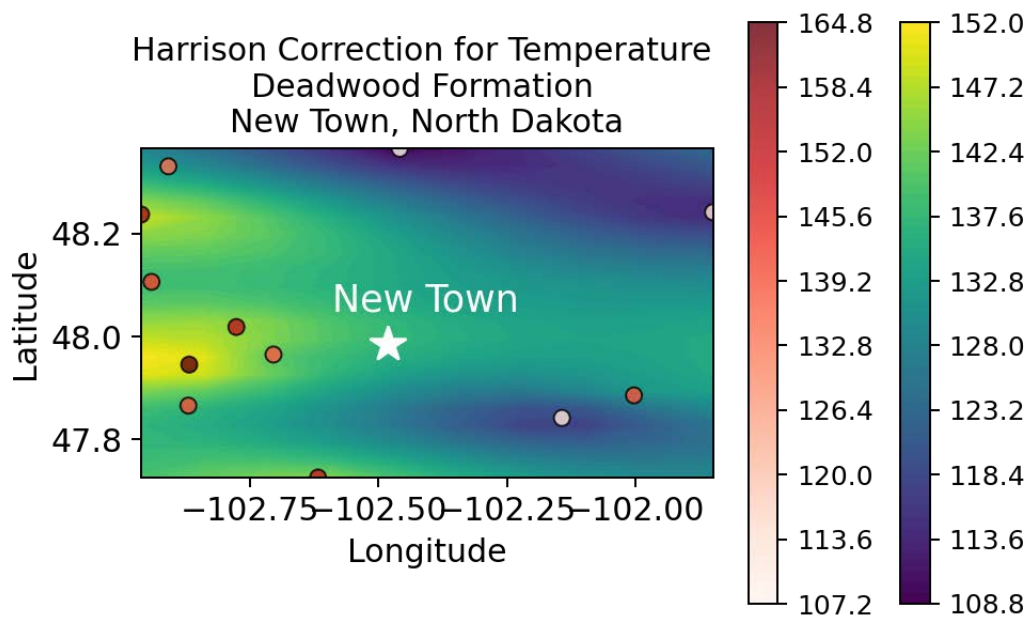


Figure 3 From 12 wells assessed with the Harrison correction in Namie et al. (2022), ordinary kriging of the Deadwood Formation indicates temperatures below 155 °C. Kriging temperatures (°) appear in the yellow-blue spectrum, while the Harrison correction temperatures from the wells appear in reds.

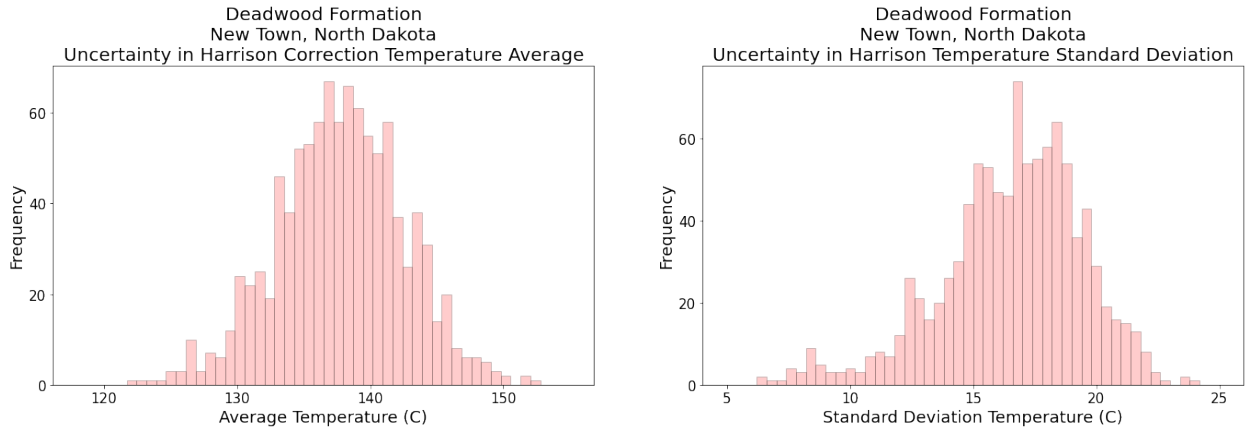


Figure 4 Bootstrap simulation statistics of the Harrison Correction temperatures from data in Namie et al. (2022).

$$T(z) = T_0 + \sum_{i=1}^n \frac{qz_i}{\lambda_i} \quad \text{Equation 8}$$

W. D. Gosnold et al. (2012) suggests the TSTRAT calculations respect the physical properties of the subsurface, rather than relying on correlations of logs and subsequent corrections. Beneath New Town, North Dakota, Namie et al. (2022) finds a TSTRAT temperature value at the Deadwood reservoir to be 136.2°C. This TSTRAT temperature serves as the basis for an analytical model of the thermal drawdown profile for the reservoir, assuming some hydraulic stimulation takes place.

2.3 Geothermal Reservoir Simulation Parameters

Though the geothermal reservoir parameters in use for this study are not rigorous, they do provide a basis from which to modify and adapt the energy system when primary data becomes available to the investigator. In this case, GEOPHIRES, available on GitHub from the National Renewable Energy Laboratory, provides the production data based on the parameters in Table 2 (K. Beckers, 2020). Although GEOPHIRES is a techno-economic simulator, economic outcomes are not run through the software, and the temperature simulation outputs are taken to later build a matrix of power and thermal outputs based on lake temperature inputs to the TESP, Habka 4 power plant. Temperature outputs, from flow rates of 30-50 kg/sec, appear in Figure 5.

Table 2 Reservoir simulation parameters run in GEOPHIRES.

Parameter	Value	Unit
Reservoir Model	Armstead and Tester 1987	
Ramey Wellbore Model	Enabled	
Reservoir Depth	3.75	km
Well diameters	12.25	inch
Circulation Pump Efficiency	80	%
Well Separation	1000	m
Maximum Temperature	136	°C
Injection Temperature	90	°C
Drawdown Parameter	$4.26 \cdot 10^{-5}$	kg/s/m ²
Thermal Conductivity	2.5	W/m/K
Density	2700	kg/m ³

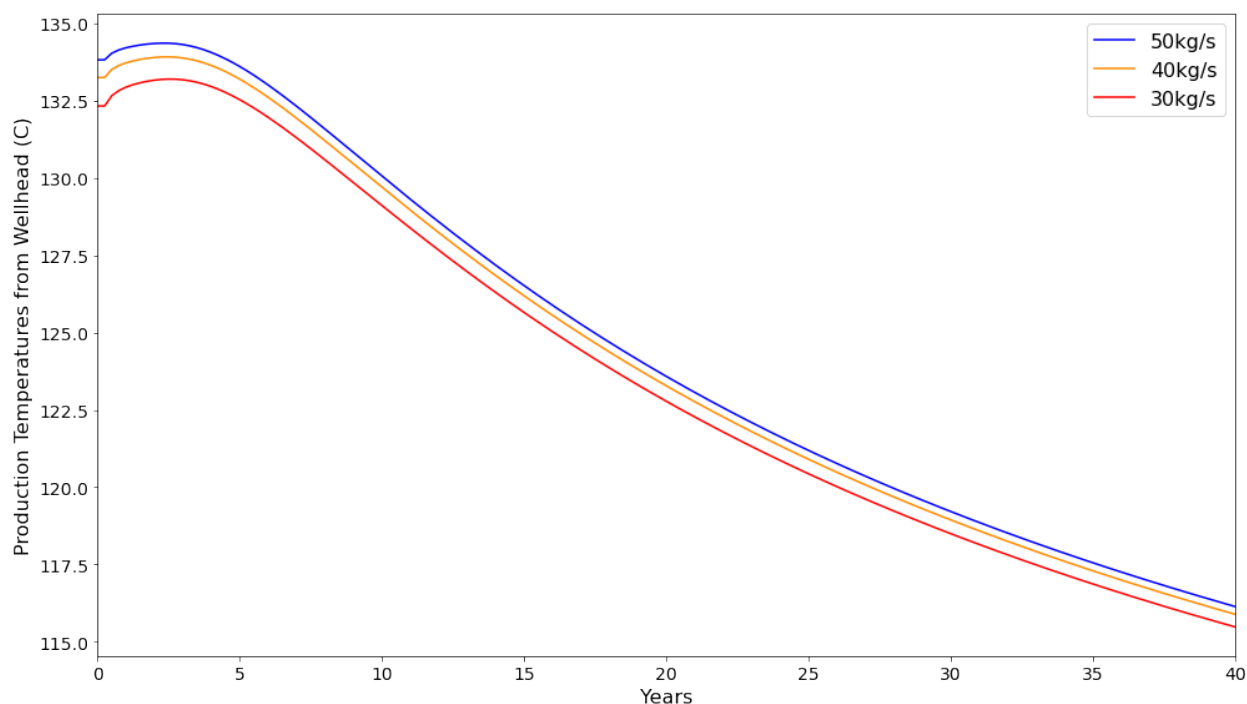


Figure 5 Temperature outputs from GEOPHIRES, based on the Armstead & Tester (1987) equation, across three flow rates.

Lake Sakakawea, a part of the Missouri River, changes temperatures seasonally. These seasonal temperature changes will affect the production capacity of a power plant. The temperatures in this case are originally drawn from surface information on seatemperature.info, (n.d.) Since these are only surface temperatures, the maximum is reset to 5.1° for this study, assuming that fluids can be drawn from depths of the Lake less influenced by solar gain variation.

2.4 Building Thermal Demand Model of New Town, North Dakota

The heating demand characterization follows preliminary methods from Dalla Rosa et al. (2012). There are today approximately 960 occupiable structures in New Town (OpenStreetMap, 2021). The majority, around 860, are residential housing units, primarily single family detached homes (Figure 6). There are several secondary schools, a college, retail, healthcare centers, public service buildings, and light manufacturing facilities within the municipal limits. Using the Commercial Building Energy Consumption Survey (CBECS) and Residential Energy Consumption Survey (RECS), the annual energy demands by region are applied to each building polygon (Figure 7), amounting to about 45.1GWh of heating (Energy Information Administration, 2016, 2018). There are no natural gas utilities in the service area and the primary heating fuel is propane. Future refinements of the energy load are possible using the National Renewable Energy Laboratory load profile inventories in ResStock and ComStock (National Renewable Energy Laboratory, 2021a, 2021b), or using other building simulation tools.

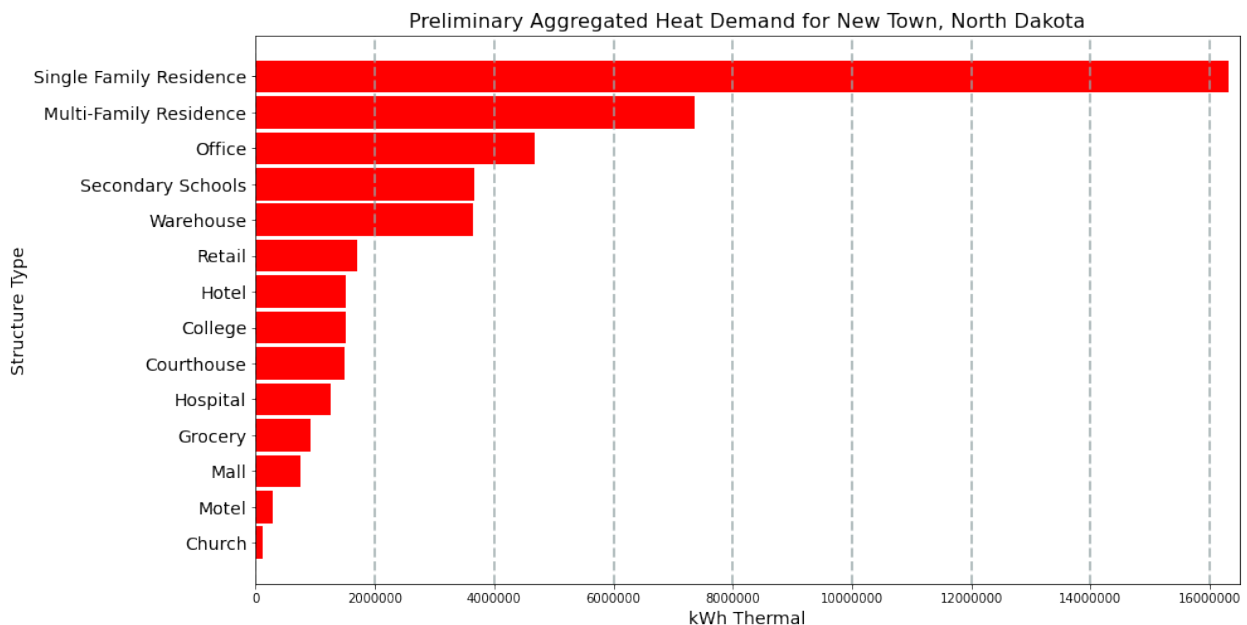


Figure 6 Preliminary aggregated demand by structure type for all buildings in New Town, North Dakota.

Although MHA Nation has seen a recent influx of dollars from shale gas exploitation across the Williston Basin, the poverty level of Mountrail County, where New Town rests, remains high (Statewide Longitudinal Data System, 2021). Since the 2010 US Census, New Town grew by 37% and new housing construction projects are underway on the northside. Along with this new development, recent prices for consumer propane rose to \$2.27 per gallon - 91,502 Btus or \$0.084kWh, excluding taxes, for the week of 28 March 2022 (Energy Information Administration, 2022). The community is heating dominant, based on general load profiles available from National Renewable Energy Laboratory (2021) (Figure 8).

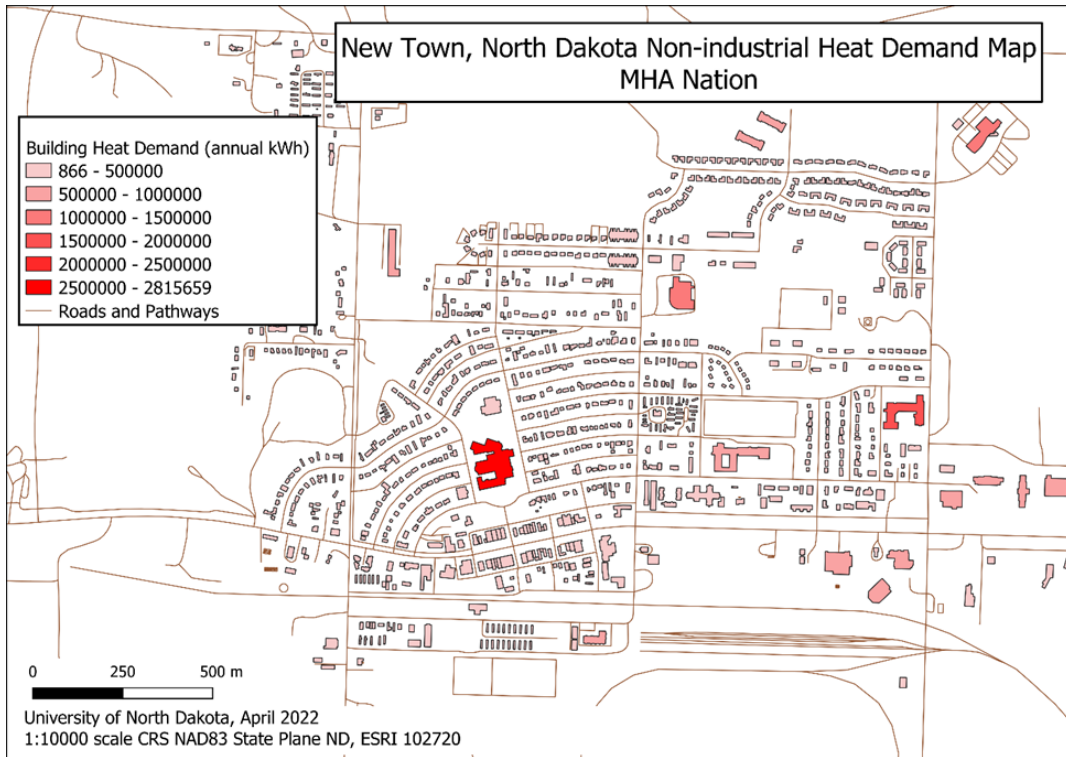


Figure 7 Preliminary heat demand map for New Town, North Dakota.

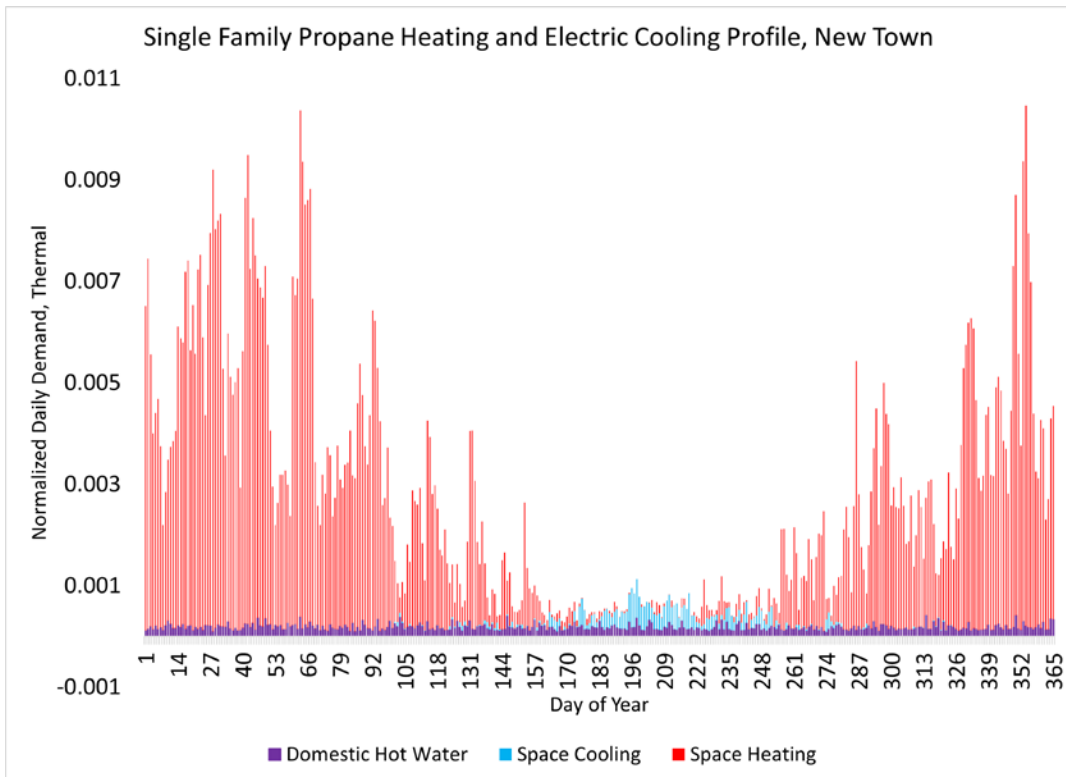


Figure 8 Typical single-family heating and cooling load profile in New Town, North Dakota (National Renewable Energy Laboratory, 2021).

2.5 Thermal Energy Network

Outputs from the power plant affect the thermal network extent. The thermal output varies with the geothermal production flow rates. To keep the thermal network extents topologically accurate, this study uses a Quantum Geographical Information System (QGIS) plugin, Comsof Heat. Comsof Heat provides static hydraulic simulation of the network using the spatial data available from OpenStreetMaps and the building energy demand model. The design constraints for the DES heat exchanger are set at 2MW_{th} and 1.5MW_{th} with a supply temperature of 55° and a return temperature of 35° , irrespective of the geothermal mass flow and feeding temperatures to the CHP-ORC.

2.6 Load Curves for CHP Performance

The CHP-ORC requires the user to develop a normalized load curve. This load curve will determine the efficiency factor of the CHP-ORC up to the point of heat exchange with the district system. Using Ladybug Tools (Sadeghipour Roudsari et al., 2013), a building simulation for the western portion of New Town isolates the anchor loads for heating and cooling demand – namely New Town High School and the surrounding residential area, representative of the entire town’s load profile (Figure 9). In aggregate the load curve for the district appears in Figure 10. Normalizing this load curve provides a meaningful input for CHP-ORC cooling control. Seasonal levels of heat demand will impact the available waste heat. When this waste heat is not put to use at the plant, there is a likely drop in efficiency.

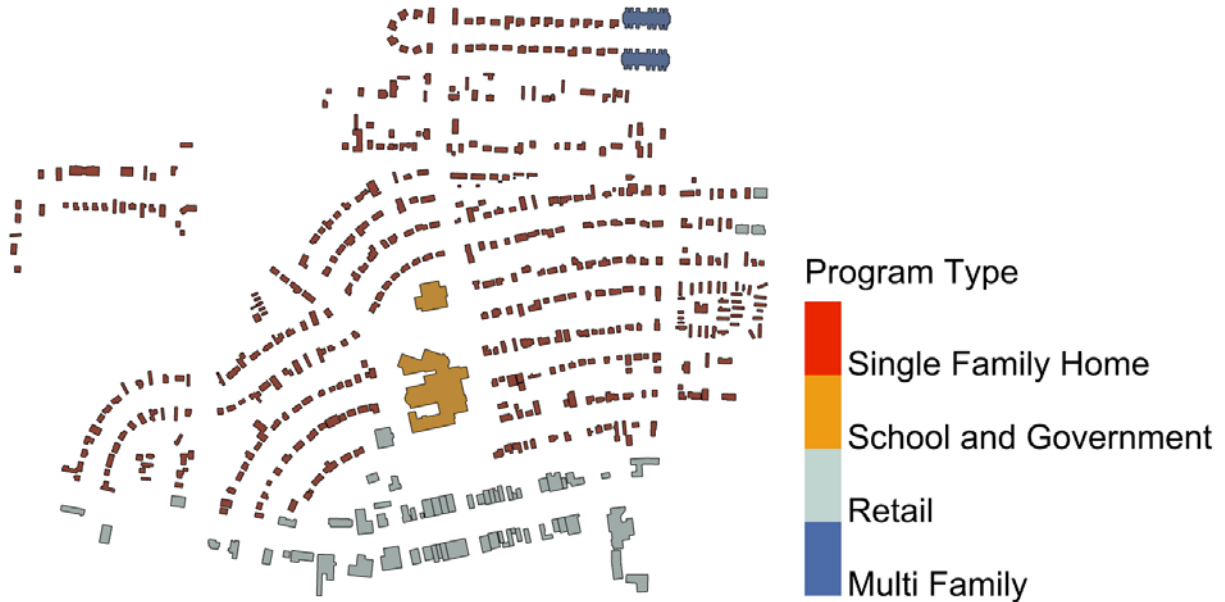


Figure 9 Area of preliminary building simulation, containing 671 structures, to derive and confirm heating and cooling load profiles.

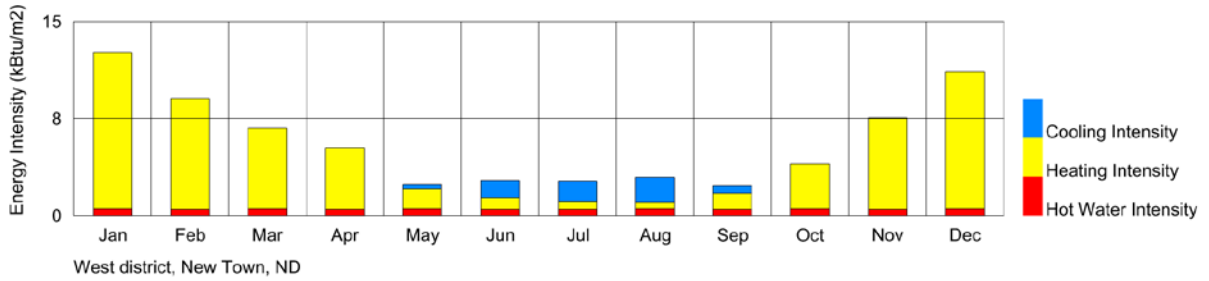


Figure 10 Preliminary aggregated building simulation outcomes from the western portion (671 structures) of New Town, North Dakota.

The seasonality of heat demand for New Town coincides with higher lake temperatures (Figure 11). Increased lake temperature generally leads to decrease in ORC power cycle efficiency, meaning with the same amount of heat input, less power is generated. At the same time, however, demand is reduced, thus more heat input is available for the power cycle leading to higher power supply.

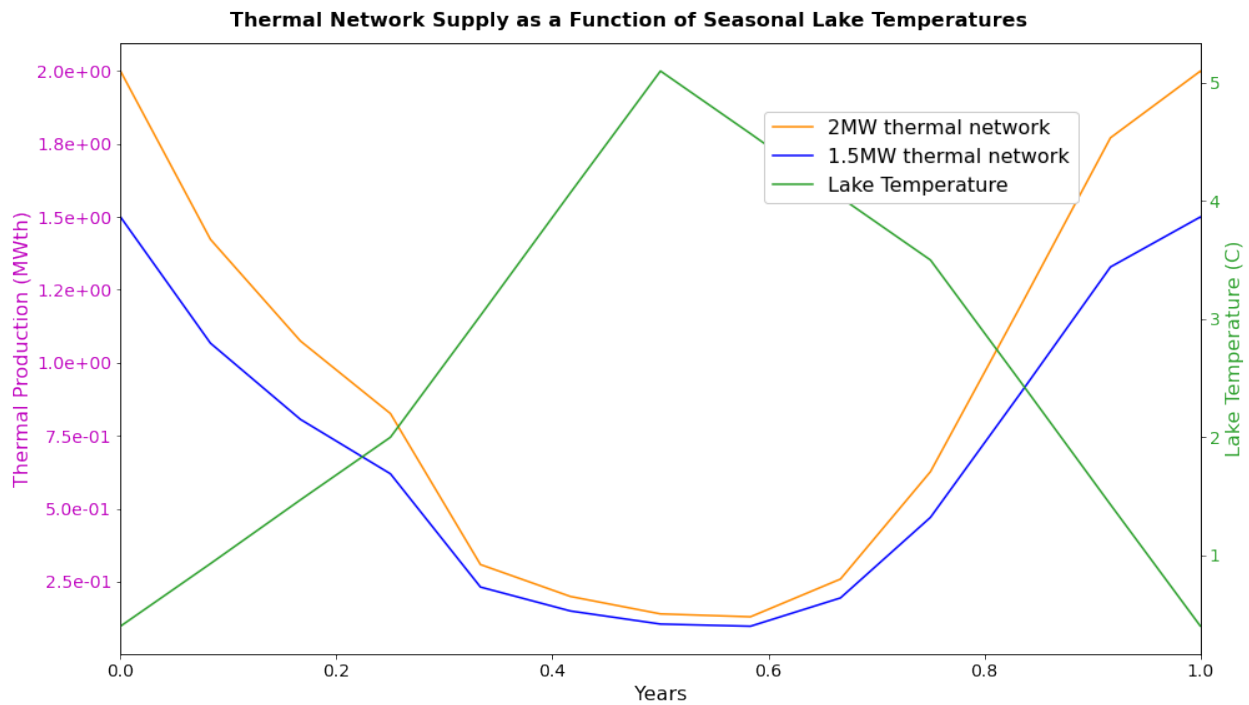


Figure 11 Thermal production as a function of the Lake Sakakawea seasonal temperatures.

3. Results

This section introduces the results of the power plant, the thermal energy network, and the specific energy allocations for the components. These energy allocations are affected by the

different plant layouts, including network extents. Power and heat generation vary with these configurations over the lifetime of operations, with specific impacts on the overall efficiencies.

3.1 Power Plant Production Capacity

Electricity supply is shown in Figure 12 and Figure 13 over the production lifetime of 40 years for a 1.5MW_{th} and a 2MW_{th} district design. For both designs the geothermal brine mass flow has been varied from 30 kg/s to 50 kg/s. Generally, several boundary conditions affect the electricity supply:

- 1.) The decline of the geothermal brine temperature.
- 2.) The seasonality of New Town, North Dakota
- 3.) A strengthening of power allocation oscillations over time.

First, supply follows the decline in the geothermal brine temperature because the heat input to the power cycle declines over time, assuming the minimum reinjection temperature constraint remains in place. The decline is visible for all geothermal mass flow regimes. As expected, higher geothermal brine mass flow increases the power provision, making more thermal input available to the ORC power cycle.

Second, a strong seasonality across each year affects the heat demand and lake temperature. A decrease in heat demand should increase the electricity generation, but the lake temperature increase inhibits some of these benefits, dampening the maximum potential of summer power production. In winter, the reduction of power due to increasing heat demand is somewhat offset by the higher efficiency of the cycle with a lower temperature in the lake.

Third, the range of seasonal oscillations from rather low fluctuation in the beginning of the operation to high fluctuation up to 250 kW at the end of life affects the power supply. Year over year the heat demand curve changes between a peak in the winter and lows in the summer, relative to the thermal energy available from the geothermal brine increases. Therefore, the fluctuations amplify with larger thermal network demand, as seen in the 2MW_{th} DES in comparison to the 1.5MW_{th} test case.

Looking at the power production in the two different thermal systems, the 2.0MW_{th} district provides a maximum generation of $1,113.7\text{kW}_{\text{elec}}$, $853.2\text{kW}_{\text{elec}}$, and $565.6\text{kW}_{\text{elec}}$, which is slightly lower than the generation of $1,118.2\text{kW}_{\text{elec}}$, $914.7\text{kW}_{\text{elec}}$, and $632.1\text{kW}_{\text{elec}}$ in the 1.5MW_{th} heat demand case.

3.2 Electricity and Heat Generation

Electricity generation decreases with the decreasing temperatures of fluids from the geothermal wells. The lower boundary of the brine temperature, set at 90° , is an important constraint. With this limitation, the electricity generation per month ranges from $79\text{MWh} - 421\text{MWh}$ and $289 - 883\text{MWh}$ for the 2MW_{th} and 1.5MW_{th} DES coupling, respectively. The total electricity generation is $148\text{GWh} - 292\text{GWh}$ for each scenario over 40 years (Figure 14). There is very little difference in the total electricity generation for either design case, as a consequence of low efficiency factors for ORC power plants.

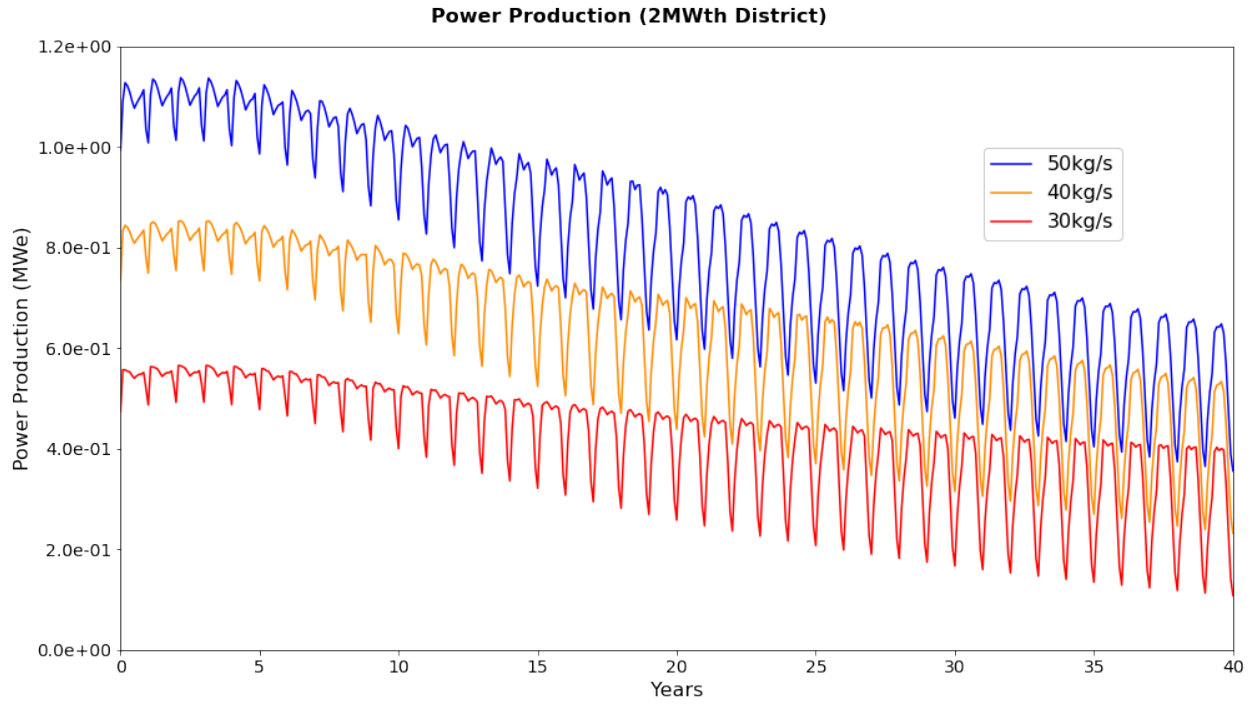


Figure 12 Power production as a function of the Lake Sakakawea seasonal temperatures using a 2MW thermal network.

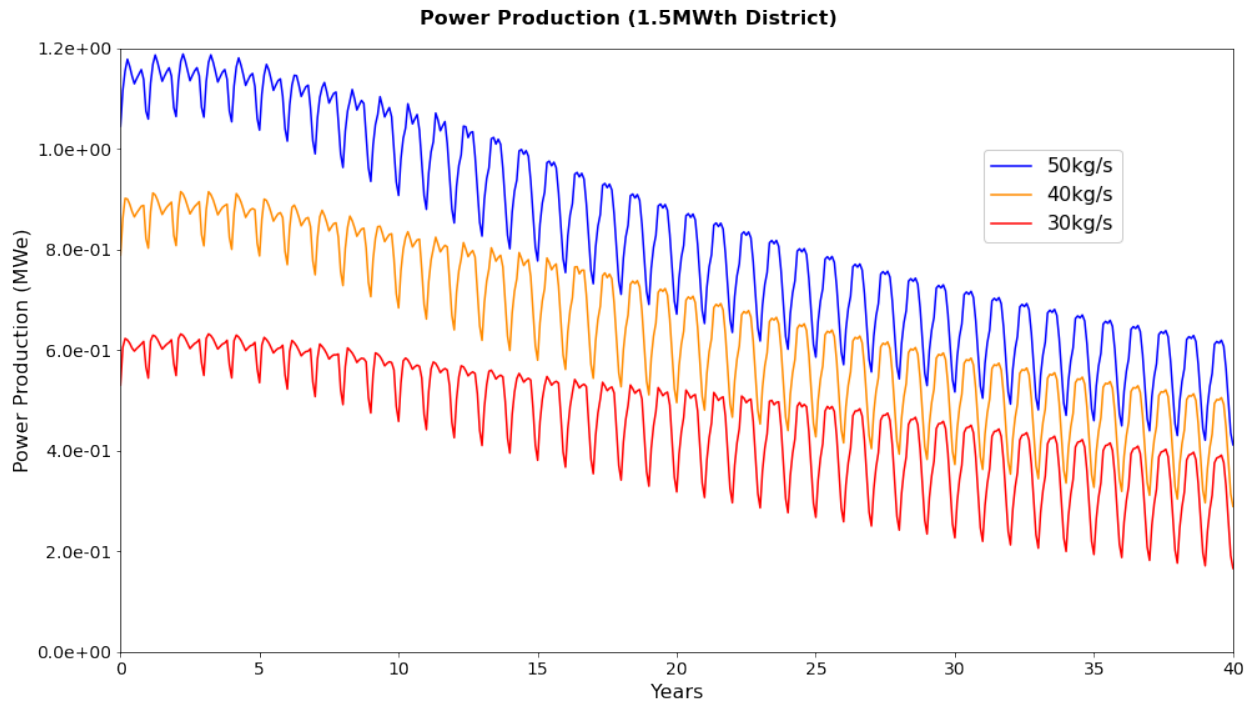


Figure 13 Power production as a function of the Lake Sakakawea seasonal temperatures using a 1.5MW thermal network.

By the end of December 2021, North Dakota electricity rates were among the lowest in the nation, at \$0.094/kWh (Energy Information Administration, 2022). In today’s dollars, the sales from electricity at the CHP-ORC amount to \$13,888,218 – \$27,429,012 over the plant lifetime. Assuming no emissions from the geothermal CHP-ORC, the CO_{2e} emissions mitigated by the electricity would range from 65,643 – 129,644 total metric tons taken off the Midwest Reliability Organization – the regional grid (US Environmental Protection Agency, 2021).

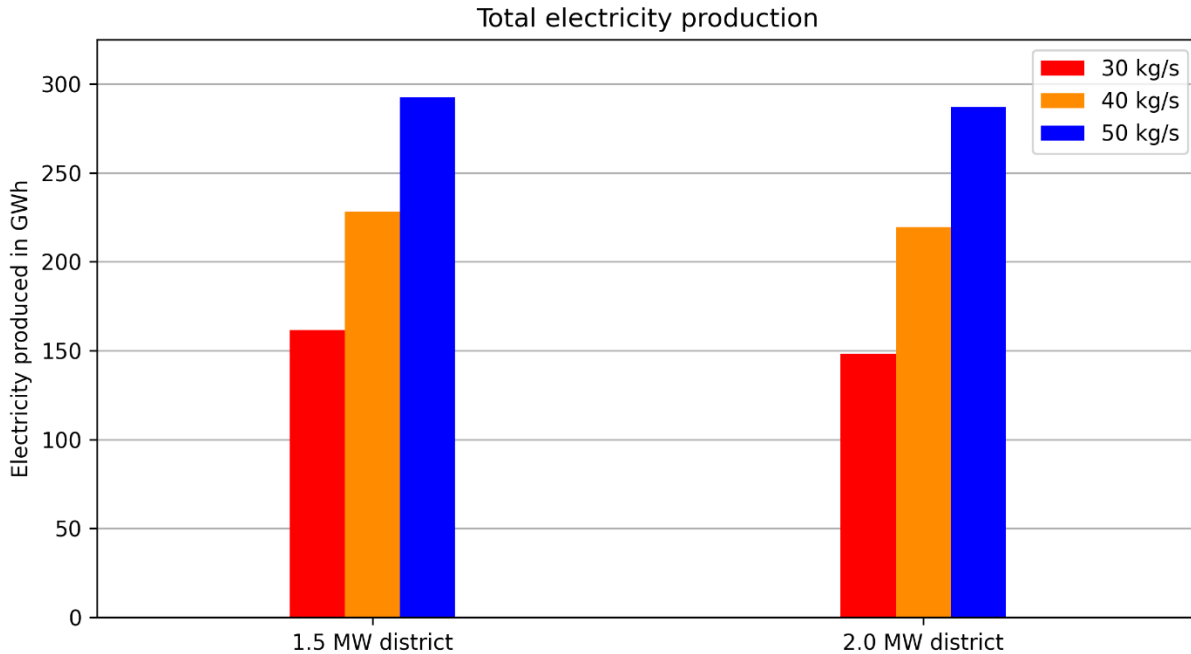


Figure 14 Total electricity generated during 40-year lifetime of plant.

Thermal availability differs slightly from the heat demand met across the network. This variation results from heat losses across the pipe infrastructure. Thermal availability to the network varies by topology. The viability of the thermal network is often a function of the saleable quantity of heat for the service area. In these scenarios, the consumption only varies with the design capacity – either 2MW_{th} or 1.5MW_{th} – of the district energy system.

For the 2MW_{th} and 1.5MW_{th} DES, the average annual thermal demand is 2,522 MWh and 1,739 MWh, after heat losses. Heat losses to ground are 21% and 18% for both the 2MW_{th} and 1.5MW_{th} scenarios. At \$0.084kWh, excluding taxes, for the week of 28 March 2022 (Energy Information Administration, 2022), the saleable amount is worth \$211,848 or \$146,076 of propane sales per year with a carbon dioxide equivalent (CO_{2e}) of 522 – 360 metric tons annually (US Environmental Protection Agency, 2015).

3.3 Thermal Network Extents

Thermal network extents for the two thermal supplies, 2MW and 1.5MW, result in pipe lengths of 13,728m and 7,322m (Figure 15). As proven, the longer the thermal network, the greater the heat losses will be – all else being equivalent. Network extents also result in different pipe diameter requirements and heating offsets. Two government buildings, a public works garage and the New Town High School, serve as the anchor loads for the thermal network. Anchor loads

are prioritized and are therefore the last structures to lose service across the thermal network. There are 100 or 44 buildings connected for the 2MW_{th} and 1.5MW_{th} scenarios, respectively.

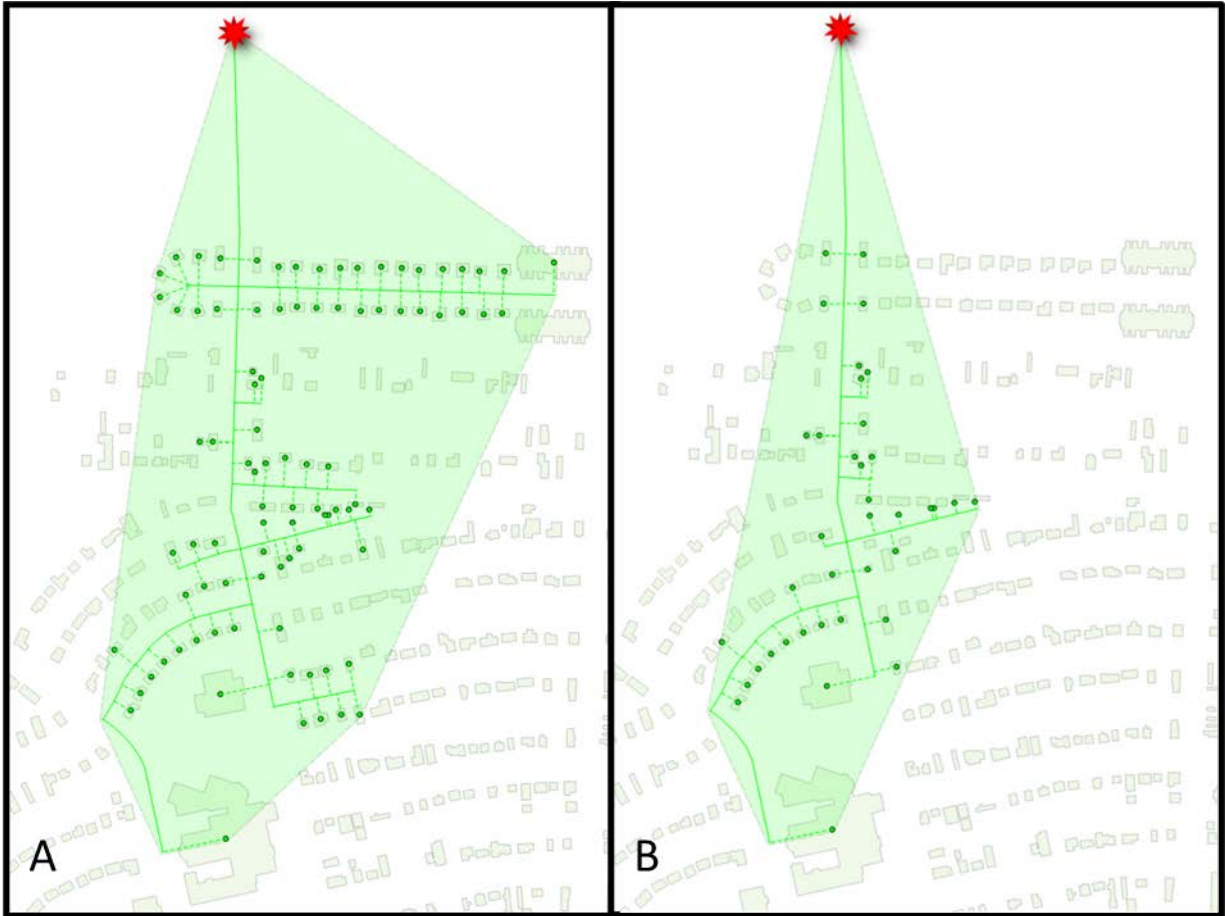


Figure 15 Network extents for the thermal energy system, augmenting the geothermal CHP-ORC in New Town. The red star indicates the power plant location. The extent of the network relates directly to the CHP-ORC heat exchanger design, either 2MW_{th} (18a) or 1.5MW_{th} (18b).

3.4 Efficiency

Regarding efficiency, Figure 16 and Figure 17 show the results for the 2MW_{th} and 1.5MW_{th} design respectively. The yearly production values better indicate the trends, instead of showing the seasonal oscillation of monthly values. With lower mass flows in the geothermal brines there are higher overall efficiencies. There is indeed lower electricity production for low-efficiency ORC power plants. By comparison, the DH system is highly efficient, 100% in these simulations since the heat exchanger is an adiabatic component. This difference in efficiencies directly affects the behavior of allocation between the electrical and thermal energy.

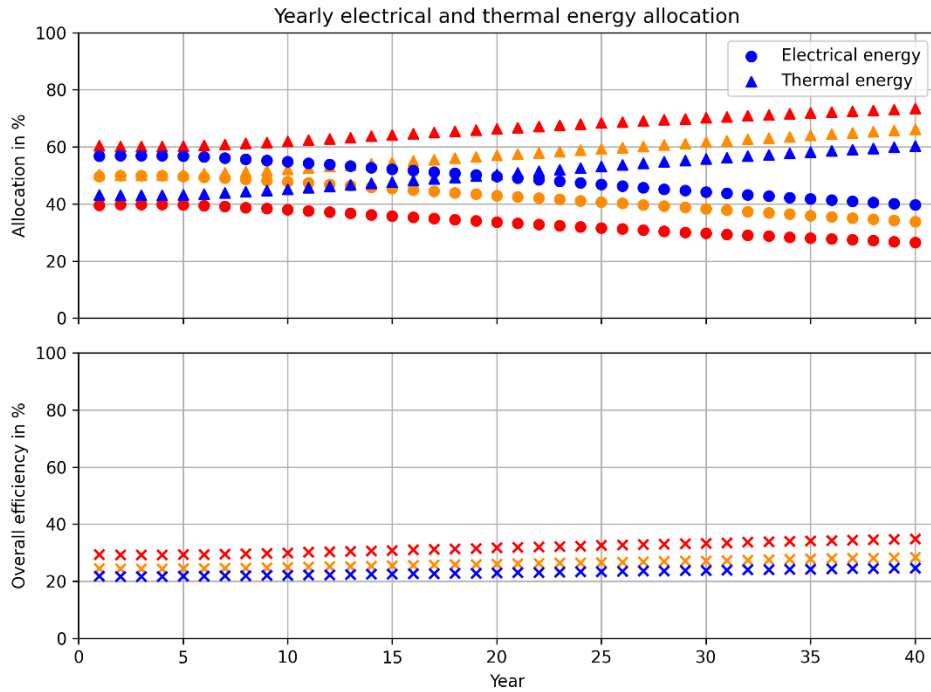


Figure 16 Allocation of yearly electrical and thermal energy provision with yearly overall CHP-ORC efficiency connected to a 2 MW thermal network. The shades indicate the mass flow (50 kg/s blue, 40 kg/s orange, 30 kg/s red).

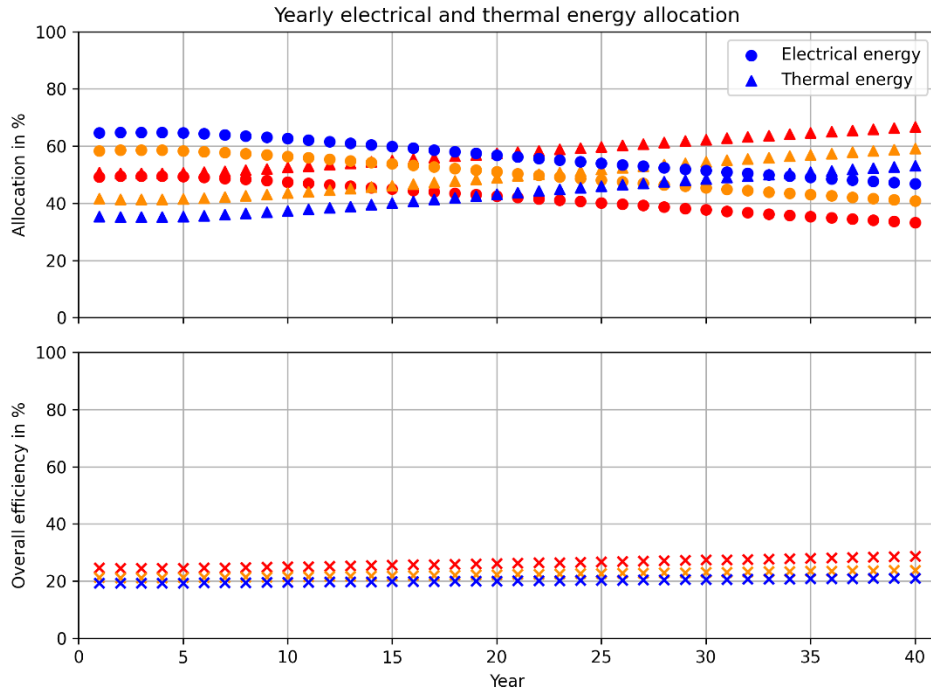


Figure 17 Allocation of yearly electrical and thermal energy provision with yearly overall CHP-ORC efficiency connected to a 1.5 MW thermal network. The shades indicate the mass flow (50 kg/s blue, 40 kg/s orange, 30 kg/s red).

The overall efficiency increases over time due to the decline in electricity production. Generally, the electricity efficiency of the ORC power cycle ranges from up to 13.5% at the beginning of the operation period to around 10% at the end of the lifetime (Figure 18). This is also seen in the allocation of heat and electricity to total production. The change is especially visible in the 2MW_{th} design, where, for example in the 30 kg/s case 60% of energy output in year one is heat and 40% is electricity. In year 40 about 75% is allocated to heat and only 25% to electricity. In year one, the 50 kg/s case starts with a little bit less than 60% electricity allocation and in year 40 the ratio inverted. The change is less extreme for the 1.5MW_{th} design. As expected, electricity allocation is generally higher in this setup with the change in allocation being less extreme.

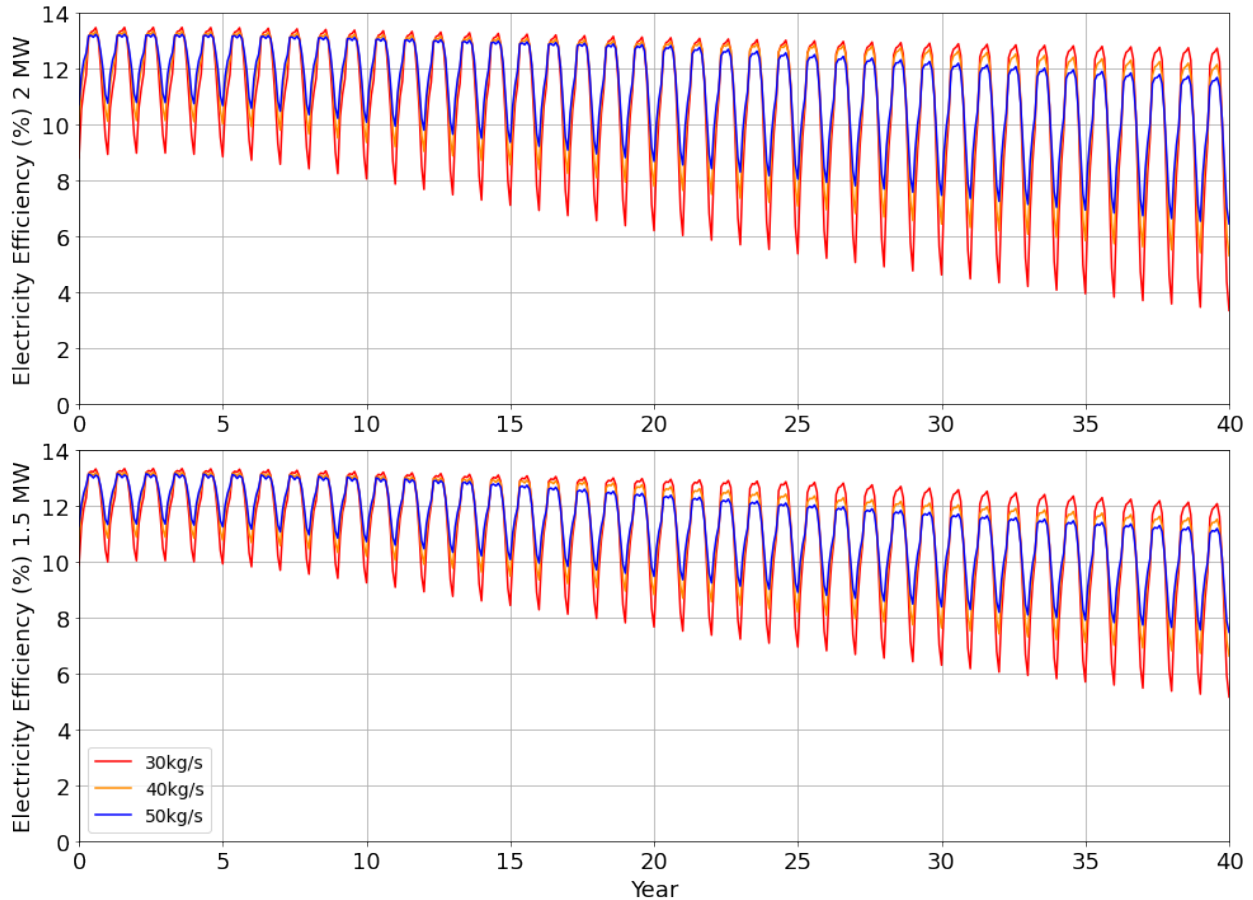


Figure 18 Electricity production efficiency of the ORC over the lifetime of the operation.

4. Discussion

In the area of New Town, North Dakota, there are hundreds of oil and gas wells. Few of these wells reach to the depth necessary to achieve efficient power generation through an ORC. Observers of the energy transition note the importance of including traditionally disadvantaged populations in technical assistance and labor reskilling programs. The residents of New Town, some of whom are MHA Nation members, certainly fall into this category. As an energy tribe, rich in oil and gas resources, MHA Nation is uniquely positioned to take advantage of geothermal resources in the Williston Basin. This paper presents a preliminary methodology for

weighing the heat and power potential within the likely temperature and flow ranges of future geothermal wells reaching the Deadwood Formation.

4.1 Income Versus Emissions Mitigation

Results indicate a potential range of power capacities of $108\text{kW}_{\text{elec}} - 1.2\text{MW}_{\text{elec}}$ depending on the achievable flow rates. Simultaneously, this ORC has the potential to provide 2.0MW_{th} or 1.5MW_{th} in peak heating capacity, for annual demands between 2,522MWh and 1,739MWh. Total potential energy offset by the installation has a value ranging from \$22,362,138 - \$33,272,052 in 2022 dollars. Selecting a system may not strictly align with the monetary return on investment, however. For these same dollar ranges, the $\text{CO}_{2\text{e}}$ emissions mitigation ranges from 86,523 – 144,044 metric tons. The earnings for each ton of carbon emissions reduction is \$258 for the 2MW_{th} DES while the small 1.5MW_{th} configuration only earns \$230 per metric ton. The dollars earned for offsetting heating emissions are much greater than those earned for offsetting the equivalent electricity grid emissions.

4.2 Future Work and Limitations

There is room to improve these preliminary works. Additional possibilities include the investigation of different working fluids. Lower temperature heat pump enabled thermal energy networks could be of interest from a thermodynamic and economic perspective. For this, a second turbine could be integrated in the cycle instead of the DH heat exchanger, where the separate condenser provides heat to the network at a low temperature. These operations could leverage cooling or heating supply where necessary with heat pumps. Using the thermal network instead of the lake as a cooling option for the ORC power cycle without topological modifications, for example to provide 30° supply and 15° return temperatures, heavily diminishes the power production. The backpressure from the condenser robs the turbine pressure gradient and the cycle quickly renders itself useless. The twin turbine configuration may ameliorate this problem.

Other cascading use opportunities exist for the thermal network. In this case, the supply temperature is a design constraint, making return temperatures consistent. Dynamic hydraulic simulation could invite the use of intermittent industrial process heat (e.g., greenhouses, recreational pools, among others). Interpolation tables for the return temperatures may be helpful in processing these demand profiles in TESP, resulting in more accurate production values.

The geothermal reservoir model could also improve. There is great potential to couple numerical modeling simulations to the power plant instead of analytical variants, as shown in this study. Numerical models at depth could be computationally intensive, however, working through iterations of power plant inputs and the reinjection impacts on the reservoir. A more useful approach may again be interpolation and lookup tables to avoid potential convergence problems.

5. Conclusion

There are many energy service companies, oil and gas companies, and startup companies attempting to pivot their operations towards low-carbon emission geothermal operations. The energy densities for the low- to moderate-enthalpy systems usually require the implementation of a binary power cycle. A Habka-4 ORC can improve the operational efficiency of the CHP. If the Habka-4 feeds a low-temperature thermal network, building owners across the network may

reduce annual fuel expenditures, reduce primary energy consumption, and lower the emissions intensity of their heating needs.

Using Thermal Engineering Systems in Python (TESPy) for the ORC simulation and Comsol Heat for the thermal network topology and assessment, this study indicates that small scale geothermal generator sets are operationally cost effective when combining them with district energy system. Though there is additional work to do in terms of capital costs and other economic assessments, the operational conditions appear profitable. Additional work is necessary for optimal selection of the refrigerants or hydrocarbons in the CHP-ORC.

References

- Armstead, H. C. H., & Tester, J. W. (1987). *Heat mining*. New York, New York: Methuen Inc. Retrieved from <https://www.osti.gov/biblio/6729842>
- Averfalk, H., Benakopoulos, T., Best, I., Dammel, F., Engel, C., Geyer, R., et al. (2021). *Low-temperature district heating implementation guidebook*. Stuttgart: Fraunhofer Verlag. Retrieved from <http://publica.fraunhofer.de/dokumente/N-640204.html>
- Beckers, K. (2020). *NREL/GEOPHIRES-v2*. Python, National Renewable Energy Laboratory. Retrieved from <https://github.com/NREL/GEOPHIRES-v2>
- Beckers, K. F., & McCabe, K. (2019). GEOPHIRES v2.0: Updated geothermal techno-economic simulation tool. *Geothermal Energy*, 7(1), 1–28. <https://doi.org/10.1186/s40517-019-0119-6>
- Blackwell, D., & Richards, M. (2004). Calibration of the AAPG geothermal survey of North America BHT database. Presented at the AAPG Annual Meeting, Dallas, Texas. Retrieved from <https://www.searchanddiscovery.com/abstracts/html/2004/annual/abstracts/Blackwell.htm>
- Collins, J. (1959). The history of district heating. *District Energy OnSite*, (June, 2009). Retrieved from http://www.verenum.ch/Dokumente/1959_Collins_History.pdf
- Dalla Rosa, A., Boulter, R., Church, K., & Svendsen, S. (2012). District heating (DH) network design and operation toward a system-wide methodology for optimizing renewable energy solutions (SMORES) in Canada: A case study, 45(1), 960–974. <https://doi.org/10.1016/j.energy.2012.06.062>
- Energy Information Administration. (2016). Table C30. Natural gas consumption and conditional energy intensity by climate region, 2012. Retrieved February 17, 2021, from <https://www.eia.gov/consumption/commercial/data/2012/c&e/cfm/c30.php>
- Energy Information Administration. (2018). Table CE1.3 Summary annual household site consumption and expenditures in the Midwest—totals and intensities, 2015. Retrieved from <https://www.eia.gov/consumption/residential/data/2015/c&e/pdf/ce1.3.pdf>
- Energy Information Administration. (2022, January). North Dakota: State profile and energy estimates. Retrieved April 23, 2022, from <https://www.eia.gov/state/data.php?sid=ND>
- Frederiksen, S., & Werner, S. (2013). *District Heating and Cooling* (1st ed.). Lund, Sweden: Studentlitteratur.

- Gosnold, W., Crowell, A., Keller, K., Brunson, D., Tyler, L., Nwachukwu, F., et al. (2017). Concept for a distributed baseload binary power network. In *Geothermal Resources Council Transactions*. Davis, California. Retrieved from <https://publications.mygeoenergynow.org/grc/1033840.pdf>
- Gosnold, W. D., McDonald, M. R., Klenner, R., & Merriam, D. (2012). Thermostratigraphy of the Williston Basin. *GRC Transactions*, 36, 663–670.
- Habka, M., & Ajib, S. (2014). Investigation of novel, hybrid, geothermal-energized cogeneration plants based on organic Rankine cycle. *Energy*, 70, 212–222. <https://doi.org/10.1016/j.energy.2014.03.114>
- van der Heijde, B., Vandermeulen, A., Salenbien, R., & Helsen, L. (2019). Integrated Optimal Design and Control of Fourth Generation District Heating Networks with Thermal Energy Storage. *Energies*, 12(14). <https://doi.org/10.3390/en12142766>
- Jebamalai, J. M., Marlein, K., & Laverge, J. (2020). Influence of centralized and distributed thermal energy storage on district heating network design. *Energy*, 117689. <https://doi.org/10.1016/j.energy.2020.117689>
- Lövin, I., & Andersson, M. (2015). How Sweden shows decoupling GDP growth from CO2 emissions is possible. *World Economic Forum*. Retrieved April 25, 2022, from <https://www.weforum.org/agenda/2015/06/how-sweden-shows-decoupling-gdp-growth-from-co2-emissions-is-possible/>
- Lund, H., Werner, S., Wiltshire, R., Svendsen, S., Thorsen, J. E., Hvelplund, F., & Mathiesen, B. V. (2014). 4th generation district heating (4GDH): Integrating smart thermal grids into future sustainable energy systems. *Energy*, 68, 1–11. <https://doi.org/10.1016/j.energy.2014.02.089>
- Namie, S., Alamooti, M., Onwumelu, C., & Ngobidi, N. (2022). Geothermal in North Dakota's sedimentary basin: Analysis of the Deadwood Formation. Presented at the Geothermal Rising Conference, Reno, Nevada: Geothermal Rising.
- National Renewable Energy Laboratory. (2021a). ComStock - NREL. Retrieved April 23, 2022, from <https://comstock.nrel.gov/>
- National Renewable Energy Laboratory. (2021b, October 28). ResStock Data Viewer. Retrieved November 7, 2021, from https://resstock.nrel.gov/dataviewer/?datasetName=vizstock_resstock_tmy3_release_1_by_state
- OpenStreetMap. (2021). OpenStreetMap - New Town, North Dakota. Retrieved October 22, 2021, from <https://www.openstreetmap.org/>
- Sadeghipour Roudsari, M., Pak, M., & Smith, A. (2013). Ladybug: a parametric environmental plugin for grasshopper to help designers create an environmentally-conscious design. In *Proceedings of the 13th International IBPSA Conference*. Lyon, France. Retrieved from http://www.ibpsa.org/proceedings/BS2013/p_2499.pdf
- seatemperature.info. (n.d.). Water temperature in Lake Sakakawea today. Retrieved April 9, 2022, from <https://seatemperature.info/lake-sakakawea-water-temperature.html>
- State Historical Society of North Dakota. (2020). American Indians of North Dakota. Retrieved October 31, 2021, from <https://www.ndstudies.gov/gr4/american-indians-north-dakota>

- Statewide Longitudinal Data System. (2021). Insights of New Town, North Dakota: School equity. Retrieved November 4, 2021, from <https://insights.nd.gov/Education/School/SchoolImprovement/EquityReport/3100160393>
- US Environmental Protection Agency, O. (2021, July 23). Power Profiler [Data and Tools]. Retrieved June 4, 2022, from <https://www.epa.gov/egrid/power-profiler>
- Van Erdeweghe, S., Van Bael, J., Laenen, B., & D'haeseleer, W. (2018). Optimal combined heat-and-power plant for a low-temperature geothermal source. *Energy*, *150*, 396–409. <https://doi.org/10.1016/j.energy.2018.01.136>
- Werner, S. (2017). District heating and cooling in Sweden. *Energy*, *126*, 419–429. <https://doi.org/10.1016/j.energy.2017.03.052>
- White Hawk, R. (2017). Community-Scale Solar: Watt's In It for Indian Country?, *40*, 37.
- Witte, F., & Tuschy, I. (2020). TESPy: Thermal Engineering Systems in Python. *Journal of Open Source Software*, *5*(49), 2178. <https://doi.org/10.21105/joss.02178>